Chemical Research in Toxicology

Article

Cite This: Chem. Res. Toxicol. 2018, 31, 308−318

pubs.acs.org/crt

High-Fat Diets Alter the Modulatory Effects of Xenobiotics on Cytochrome P450 Activities

Natalie C. Sadler, Bobbie-Jo M. Webb-Robertson, Therese R. Clauss, Joel G. Pounds, Richard Corley, and Aaron T. Wright*

Chemical Biology & Exposure Sciences, Biological Sciences Division, Pacific Northwest National Laboratory, Richland, Washington 99352 United States

Supporting Information

ABSTRACT: Cytochrome P450 monooxygenase (P450) enzymes metabolize critical endogenous chemicals and oxidize nearly all xenobiotics. Dysregulated P450 activities lead to altered capacity for drug metabolism and cellular stress. The effects of mixed exposures on P450 expression and activity are variable and elusive. A high-fat diet (HFD) is a common exposure that results in obesity and associated pathologies including hepatotoxicity. Herein, we report the effects of cigarette smoke on P450 activities of normal weight and HFD induced obese mice. Activity-based protein profiling results indicate that HFD mice had significantly decreased P450 activity, likely instigated by proinflammatory chemicals, and that P450 enzymes involved in detoxification, xenobiotic metabolism, and bile acid synthesis were effected by HFD and smoke interaction. Smoking increased activity of all lung P450 and coexposure to diet effected P450 2s1. We need to expand our understanding of common exposures coupled to altered P450 metabolism to enhance the safety and efficacy of therapeutic drug dosing.

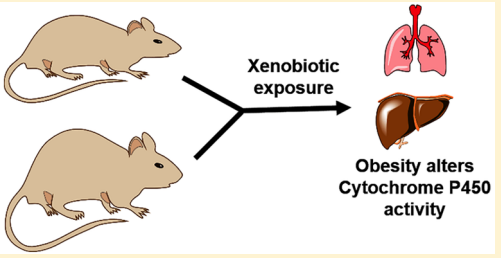

INTRODUCTION

The worldwide rate of adult obesity has doubled since 1980, with 39% of adults classified as overweight.[1] Diet induced obesity (DIO) is accompanied by chronic inflammation, oxidative stress, and increased susceptibility to a wide range of comorbidities including type 2 diabetes mellitus (T2DM), hypertension, nonalcoholic fatty liver disease (NAFLD), gallbladder disease, and some cancers.[2] Compared to individuals with normal body mass, obese individuals also have a higher risk of hepatotoxicity[3,4] and experience physiological changes that alter the pharmacokinetics (PK) and pharmacodynamics (PD) of drug metabolism.[5,6] Obesity-induced changes to PK and PD are variable and are thought to be altered by blood flow, adipose tissue distribution, microbiome composition,[7,8] and the functional status of drug metabolizing enzymes (DME).[9] Despite this knowledge, drug dosing recommendations are still primarily derived from clinical evaluation of healthy weight individuals. Obese individuals are greatly under-represented in these evaluations, thereby leading to ill-defined and potentially harmful drug dosing regimens for obese patients.[4−6,10]

Pharmaceuticals represent one class of the xenobiotics humans are exposed to daily. Others include diet-derived compounds (e.g., polyphenols, phytoestrogens, lipids, and preservatives), cleaning products, cosmetics, pesticides, air pollution, and active (first-hand) or passive (second-hand/environmental) cigarette smoke. Chemical composition, concentration, and route of exposure dictate how our cells enzymatically transform each xenobiotic to increase polarity, decrease toxicity, or derive nutrients.[2] Xenobiotics frequently undergo oxidative metabolism, an event catalyzed by cytochrome P450 monooxygenases (P450).[11] These enzymes are primarily located in the endoplasmic reticulum of a cell, but the quantity and complement of P450 are tissue specific with the highest diversity and concentration found in the liver.[12] In addition to xenobiotics, endogenous P450 substrates include cholesterol and fatty acids, the metabolism of which is crucial for a vast number of diverse cellular processes. Each P450 varies in substrate selectivity or promiscuity and can be differentially regulated.[13] For clarity, P450 are grouped into families by sequence similarity and not substrate specificity; P450 with ≥40% sequence match are grouped in numerical families, and P450 with ≥55% sequence match are grouped in alphabetical subfamilies. Individual enzymes are designated by a number that follows the subfamily letter.[12]

There is a paucity of research focused on determining the impact of multiple xenobiotic exposures on DME function. Obesity is common in modern society and is often accompanied by health complications that require medications prescribed with doses determined for nonobese individuals. Defining how DIO alters xenometabolism activities could enhance our understanding of susceptibilities to associated health risks and may lead to improved therapeutic practices.[4−6,10] With this as motivation, we implemented activity-based protein profiling (ABPP) techniques to characterize functionally active P450 in the liver and lungs of regular weight mice fed a standard diet (SD) or DIO mice fed a high-fat diet

Received: January 12, 2018
Published: April 24, 2018

DOI: 10.1021/acs.chemrestox.8b00008
Chem. Res. Toxicol. 2018, 31, 308−318

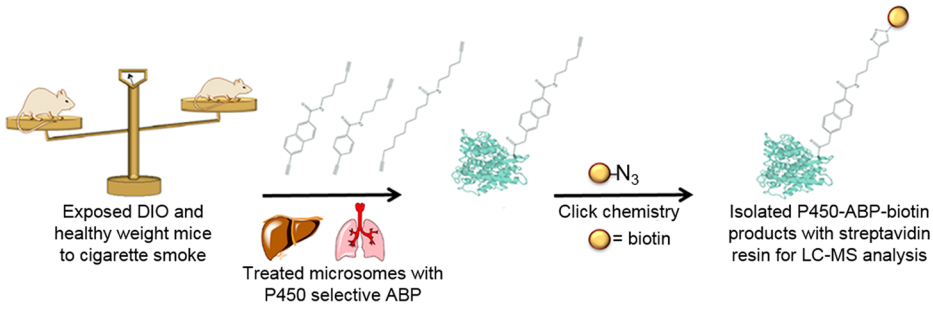

Figure 1. Activity-based protein profiling P450. High-fat diet induced obese and SD mice were exposed to active or passive cigarette smoke. Microsomes were isolated form the liver and lungs and treated with activity-based probes (ABP). Following P450 labeling, click chemistry was used to append azido biotin, and the protein-probe-biotin products were enriched on streptavidin resin. ABP targeted enzymes were trypsin digested on-resin and the resulting peptides were characterized by high-resolution LC–MS.

(HFD). In addition to diet, we evaluated the metabolic consequences of active cigarette smoke exposure (ACSE) or passive cigarette smoke exposure (PCSE), also referred to as second-hand or environmental smoke, on P450 activity profiles. Cigarette smoke was chosen as a secondary exposure because it is a common habit that leads to multiorgan exposure to a highly complex mixture of chemicals that include polyaromatic hydrocarbons, nitrosamines, aldehydes, carbon monoxide, and many others.[14] DIO and CSE often lead to oxidative stress and chronic inflammation which can increase risk factors for a variety of chronic human diseases.[15]

The P450 family is challenging to study because (1) different species have their own complement of P450, (2) genetic polymorphisms can impact function, (3 and 4) P450 expression can be constitutive or regulated by diverse mechanisms, while activity can be altered by various stimuli.[16,17] Transient post-translational modifications and ligand-based inhibition or induction govern many P450 activities, but the effects are missed by classic transcriptomic and proteomic approaches which report on abundance, but are not suited to characterize P450 activity levels.[18] Activity assays are available for a subset of P450, but in many cases, assay substrates can be metabolized by multiple P450 and so results will not reflect the activity of an individual P450. Additionally, individual activity assays are not available for all P450, so comprehensive assessment of P450 activities is not feasible. To overcome these methodological deficits, we have pioneered the use of activity-based protein profiling (ABPP) to comprehensively profile the functional activity of individual P450 enzymes within the broad complement of P450 subfamilies.[18−23] This chemoproteomic technique utilizes activity-based probes (ABP) to broadly label active P450 by exploiting the enzyme's inherent catalytic activity. These mechanisms previously described by Wright et al., include P450 catalyzed oxidation of aryl alkyne moiety to reactive ketene intermediates that inactivate the enzyme by covalent adduction, or oxidation of propynyl-bearing group to a reactive Michael acceptor and covalent adduction (probe structures found within Figure 1).[21] The ABP used for this study also included an alkyne moiety to enable CuI-catalyzed azide–alkyne cycloaddition reactions (click chemistry) for appending azido-biotin reporter tags to probe labeled enzymes for subsequent streptavidin resin enrichment and analysis by quantitative high-resolution LC–MS to characterize probe labeled P450 (Figure 1). We applied this ABPP approach to investigate the consequences of common human exposures, with a focus on the individual and confounding physiological effects of DIO and active or passive CSE on hepatic and pulmonary P450 activities.

EXPERIMENTAL PROCEDURES

Animals and Diet. Standard diet (SD) and high-fat diet (HFD) fed C57BL/6J male mice were purchased from the Jackson Laboratory (Bar Harbor, ME). Only male mice were included in this study as gender is a documented factor that influences the expression and activity of some P450,[24] and we chose to constrain variables to ensure a focused study scope. The mice were acclimated to the AALAS-accredited animal facility as well as to the nose-only restraint tubes for 1 week prior to the initiation of CSE. Feed and tap water were provided *ad libitum*, except when animals were placed in exposure tubes. All animals were observed twice daily for mortality and moribundity. All procedures were carried out with the approval of the Institutional Animal Care and Use Committees at Pacific Northwest National Laboratory. The SD diets consisted of PMI 5002 Certified Rodent Diet (PMI 5002 Rodent Diet, Richmond, IN; ∼13 kcal% fat) HFD were D12492 Rodent Diet (Research Diets Inc., New Brunswick, NJ; 60 kcal% fat) starting at 6 weeks of age and continued throughout the study. The HFD mice were fed this diet for 9 weeks prior to the start of the two-week CSE regime resulting in a significant increase in body weight compared to SD animals over the same time period (Figure 2).

Active and Passive Cigarette Smoke Exposure. Filtered tobacco cigarettes (3R4F reference cigarettes) were purchased from the University of Kentucky (Lexington, KY). Cigarette Smoke Exposure System (CSES) consisted of a monitoring and control console and two rodent exposure units fitted with a Jaeger-Baumgartner 2070i cigarette smoking machine (JB2070 CSM; CH Technologies, Westwood, NJ) modified to provide simultaneous generation of ACSE and PCSE. The NoCSE filtered air exposure unit was similar but did not include a smoking machine. The automated 30-port JB2070 CSM was set to light, smoke (2 s, 35 mL puff per minute), and eject cigarettes after 7 puffs. Puff counts were set at 7 to meet the International Organization for Standardization (4387) minimum acceptable cigarette butt length (35 mm).

Exposure concentration was monitored by the system operator primarily observing the online carbon monoxide (CO) analyzer (California Analytical Instruments, Inc., Orange, CA) and controlled by adjusting of dilution or/and siphon flows to achieve the desired target reading for the CO monitor. Additional control of the ACS particle concentration was provided using the real-time aerosol monitor (RAM, Microdust Pro, Casella Cel Ltd., Bedford, UK), and additional control of the PCS particle concentration was provided using the scanning mobility particle sizer (SMPS, 3936L76, TSI, St Paul, MN).

The dose target wet-weight total particulate matter (WTPM) and carbon monoxide exposure concentration was set for 250 WTPM/L; 250 ppm of CO and 85 WTPM/L; 250 ppm of CO for ACSE and PCSE, respectively. These target concentrations were based upon levels determined by previous studies.[14] Smoke concentration (μg

DOI: 10.1021/acs.chemrestox.8b00008
Chem. Res. Toxicol. 2018, 31, 308−318

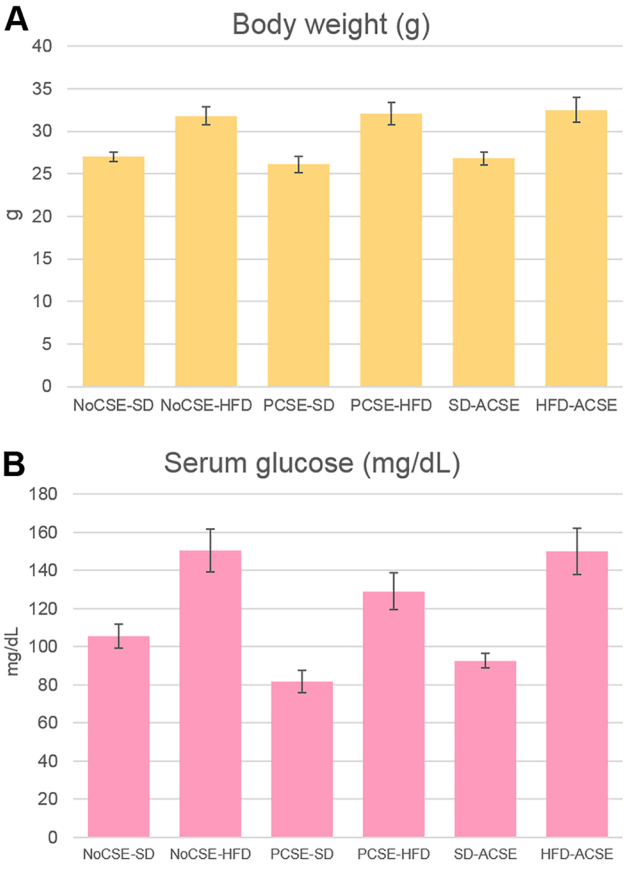

Figure 2. (A) Mean body weight, and (B) mean serum glucose at necropsy (±SE, n = 8). After 11 weeks on a SD or a HFD, the HFD mice had significantly increased (p < 0.05) body weight and serum glucose concentration compared to the SD counterparts.

WTPM/L) was determined gravimetrically from duplicate filter samples collected during the first, third, and fifth hours of the 5-h exposure period. Smoke samples were collected on Cambridge-style 47 mm glass fiber filters and mean exposure concentration was calculated from the mass collected on the filter and the total volume of air drawn through the filter, as determined by the sample time and flow rate.

Actual delivered doses were within 10% of each target, for example, 254.9 ± 10.6 WTPM/L for ACSE and 82.0 ± 6.7 WTPM/L for PCSE, with associated CO levels of 251.2 ± 6.6 ppm and 276.1 ± 8.8 ppm, respectively. Groups of SD and HFD C57BL/6J mice (15-weeks old at start of exposure) were exposed to either filtered air or cigarette smoke by nose-only inhalation exposure for 5 h per day for a total of eight exposures over 2 weeks as follows: 5 consecutive days of exposure, followed by 2 days with no exposure, then 3 days of exposure, with necropsies occurring the day following the last exposure. The target WTPM concentrations were based upon previous short-term ACSE cigarette exposure studies conducted with mice in our laboratory[14] and from preliminary range-finding studies used to establish the tolerance of SD and HFD C57BL/6 mice to the PCSE, which have lower overall particulate concentrations but a higher concentration of acutely toxic volatile components, such as CO. On the basis of these preliminary studies, CO concentrations in the exposure atmospheres were considered a limiting factor in the ability of the animals to tolerate the two-week exposure regimen with no significant overt toxicity (i.e., over 10% loss in body weight or lethality); thus, ACSE and PCSE total particulate concentrations were adjusted to achieve equivalent target CO concentrations (~250 ppm).

Carboxyhemoglobin Concentration Determination. Immediately following the last exposure, animals were anesthetized (isoflurane) and blood collected from the orbital sinus for carboxyhemoglobin (COHb) determinations using an OSM3 hemoximeter (Radiometer, Copenhagen, Denmark). Animals were removed from the exposure unit and blood collection was initiated within ~5 min. The blood samples were collected in tubes containing potassium EDTA) and placed into an ice bath until analyzed.

Tissue Collection. On the day following the last exposure, mice were euthanized with pentobarbital and exsanguinated. The liver and lungs from each mouse were collected and flash frozen and stored at −80 °C.

Serum Glucose Measurement. A glucose calorimetric assay kit (Cayman Chemicals, Ann Arbor, MA) was used as directed by manufacturer to quantify serum glucose. In short, this glucose oxidase based assay results in H_2O_2 byproduct from the enzymatic oxidation of sample glucose and subsequent enzyme reoxidation reaction. Horseradish peroxidase then catalyzes the H_2O_2 oxidation of 3,5-dichloro-2-hydroxybenzenesulfonic acid and 4-aminoantipyrine to form products with optimal absorption at 514 nm. Following incubation (37 °C, 10 min), absorbance (514 nm) was measured with a microplate spectrophotometer (SpectraMax Plus 384, Molecular Devices, Sunnyvale, CA).

ABPP Sample Preparation. Liver and lungs were razor minced, dounce homogenized in 250 mM sucrose buffer on ice, and microsomes isolated by serial centrifugation as previously described.[18] A Pierce Bicinchronic acid (BCA) kit (Thermo Fisher Scientific, Waltham, MA) was used to determine microsomal protein concentrations; assay absorbance (562 nm) was measured with a SpectraMax Plus 384. Microsomes were adjusted with 250 mM sucrose to a 1.00 mg/mL protein concentration, and duplicate samples were prepared for each animal and tissue type with 1.00 and 0.60 mL volume size for liver and lungs, respectively. One sample from each pair was prepared as a null activity (NA) control counterparts to samples prepared for profiling P450 activity.

Prior to the addition of activity-based probes, samples were treated with a requisite source of P450 reductant, nicotinamide adenine dinucleotide phosphate (NADPH; 0.63 mM). The NA controls for liver and lung samples were prepared differently due to inconclusive preliminary ABP screening by SDS-PAGE (data not shown) for the lung samples. We believe two factors led to the inconclusive results: (1) the isolated lung microsomes had substantially less protein than the liver and thereby native NADPH levels are sufficient during ABPP studies, and (2) lung tissues are documented as having less P450 expression than liver.[12] To ensure successful lung NA controls, the samples were first denatured by heat-shock (98 °C, 10 min) before ABP labeling. Alternatively, liver NA samples were not heat-shocked, but instead PBS was used in place of NADPH. All samples were then treated with an equimolar mix of the three ABPs (20 μM) and incubated (37°, 500 rpm, 60 min). To enable ABP-labeled protein enrichment, free ABP alkyne moieties were reacted with biotin-PEG3-azide (36.0 μM, 25 °C, 500 rpm, 90 min) in the presence of tris(2-carboxyethyl)phosphine (TCEP, 2.5 mM), tris[(1-benzyl-1*H*-1,2,3-triazol-4-yl)methyl]amine prepared in DMSO:*t*-butanol 1:4 (0.25 mM), and $CuSO_4$ (0.50 mM) to form triazole linked protein bound ABP-biotin complexes. To end the reaction, samples were mixed with one volume of cold MeOH, incubated on ice (10 min), centrifuged (4 °C, 10 000*g*, 5 min), and supernatants were discarded. Protein pellets were washed twice as follows: pellets were sonicated on ice in 0.50 mL of cold MeOH (10 pulses), rotated (4 °C, 10 min), centrifuged (4 °C, 10 000*g*, 5 min), and supernatants were discarded. To solubilize proteins, pellets were suspended in 0.52 mL of 1.2% sodium dodecyl sulfate (SDS) in PBS, sonicated (5 pulses), heated (90 °C, 5 min), and sonicated (5 pulses). Samples were then centrifuged (25 °C, 10 000*g*, 5 min) to pellet insoluble protein and debris, and the supernatant protein was determined by BCA assay.

To isolate the biotinylated ABP-labeled P450, 0.05 mL of prewashed Pierce streptavidin agarose resin slurry (Thermo Fisher Scientific, Waltham, MA) was added to each sample (0.36 μg of protein in 0.2% SDS in PBS) and incubated (37 °C, rotating, 4 h). Samples were then transferred to Bio-Spin columns (Biorad, Hercules, CA) and washed six times with 1.0 mL aliquots of 0.5% SDS in PBS, PBS, ultrapure water, and 6 M urea on a vacuum manifold. Next, samples were transferred to low-bind conical tubes with 1.0 mL of 6 M

DOI: 10.1021/acs.chemrestox.8b00008
Chem. Res. Toxicol. 2018, 31, 308−318

Table 1. Blood Carboxyhemoglobin (COHb) Levels after 8 Days of Cigarette Smoke Exposure

smoke	NoCSE		PCSE		ACSE	
diet	SD	HFD	SD	HFD	SD	HFD
COHb % ± SD, n = 8	1.5 ± 0.1	1.5 ± 0.1	29.6 ± 1.0[a]	29.8 ± 1.0[a,c]	29.0 ± 1.4[a]	26.4 ± 1.5[a,b]

[a] $p < 0.05$ versus NoCSE group. [b] $p < 0.05$ ACSE-SD versus ACSE-HFD group. [c] $p < 0.05$ ACSE-HFD versus PCSE-HFD group.

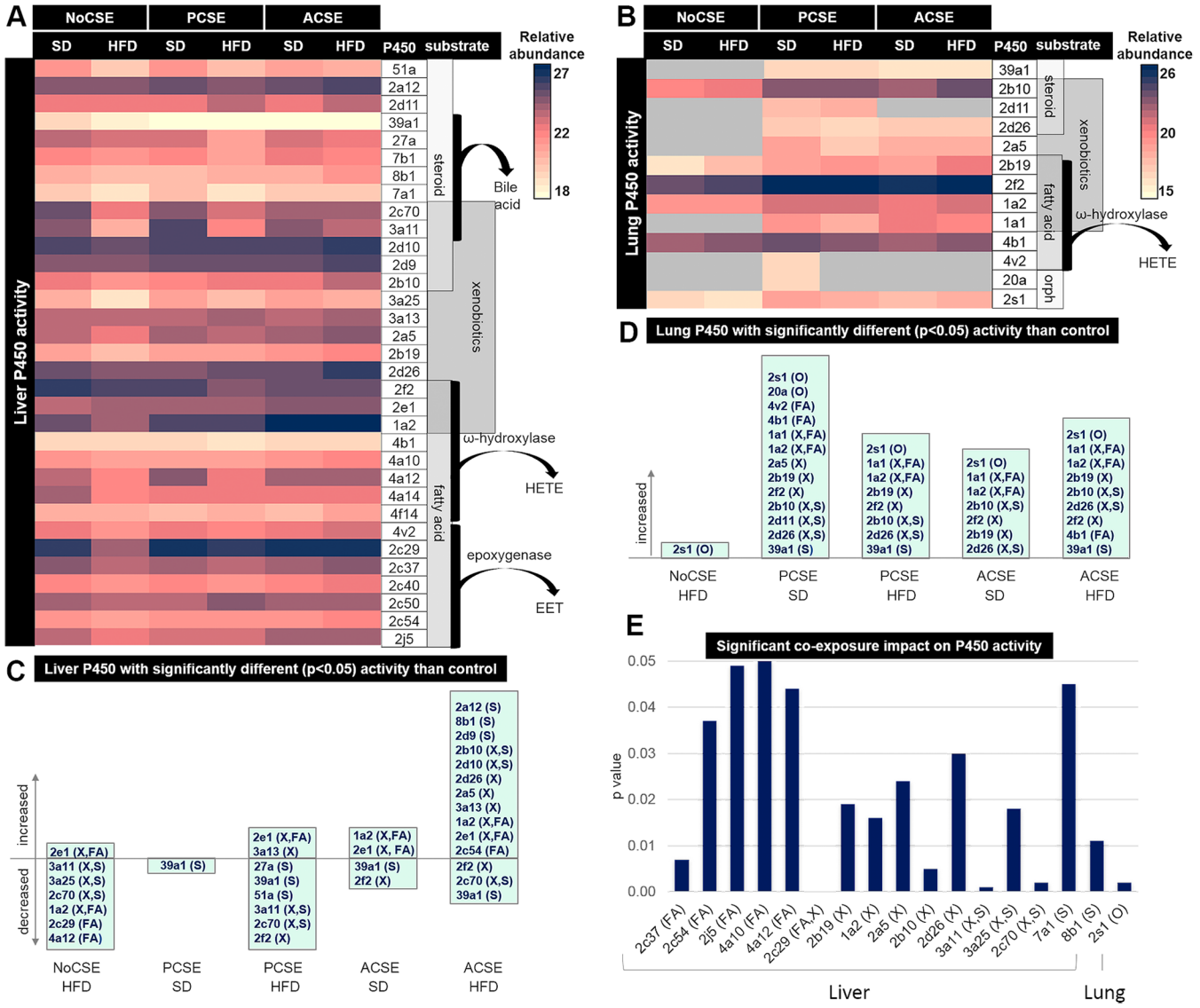

Figure 3. (A–E) Active P450 profiles for mice fed standard diet (SD) or high-fat diet (HFD) and exposed to active or passive cigarette smoke (ACSE and PCSE respectively), as determined by ABPP. (A) Liver and (B) lung heatmap columns represent each exposure group, and each row maps to a functionally active P450 as determined by probe labeling and measurement by LC–MS and the log2 transformed mean (n = 8) relative abundance. These liver data can be found in Data set S1, and lung data can be found in Data set S2. Each P450 is grouped by primary substrate (fatty acid, xenobiotic, steroid) or "orphan" if the enzyme function is still unclassified. Arrows indicate key functions and products. (C) Liver data, (D) lung data with significantly different ($p < 0.05$) relative abundance values that were increased or decreased compared to the control group (NoCSE-SD). Primary substrate(s) are included next to P450 in bar graph: fatty acid (FA), xenobiotic (X), steroid (S), or orphan (O). (E) Two-way ANOVA with Bonferonni correction performed to test the significance of the diet and smoke interaction on liver P450 and lung P450 ABPP activity. Graph only includes P450 with significant differences ($p < 0.05$).

urea, centrifuged (25 °C, 6000g, 5 min), and supernatants were discarded. Resin-bound proteins were and reduced with TCEP (2 mM, 37 °C, 1200 rpm, 30 min) in 0.20 mL of 6 M urea, alkylated with iodoacetamide (4 mM, 50 °C, 1200 rpm, 45 min), and then transferred to columns and washed six times with 1.0 mL aliquots of 6 M urea, PBS, ultrapure water, and NH_4HCO_3 (25 mM, pH 8). Proteins were digested on resin in 200 μL of NH_4HCO_3 (25 mM, pH 8) with 0.1 μg of trypsin (37 °C, 1200 rpm, 15 h). Tryptic peptides were concentrated to 40 μL by vacuum centrifugation and characterized using a Velos Orbitrap (Thermo Fisher Scientific, Waltham, MA) interfaced with a reverse-phase high-performance liquid chromatography (HPLC) system for peptide separation (LC–MS). Data were acquired for 100 min, beginning 65 min after sample injection (15 min into gradient). Spectra were collected from m/z 400 to 2000 at a resolution of 100 000 followed by data-dependent ion trap generation of tandem MS (MS/MS) spectra of the six most abundant

DOI: 10.1021/acs.chemrestox.8b00008
Chem. Res. Toxicol. 2018, 31, 308–318

ions using 35% collision energy. A dynamic exclusion time of 30 s was used to discriminate against previously analyzed ions.[18]

Proteomic Data Analysis. Peptide MS/MS spectra were searched using the mass spectra generating function plus (MSGF+) algorithm[25] against the publicly available *Mus musculus* translated genome sequence (www.uniprot.org; September 2013 collection). A minimum of six amino acid residues were required for peptide analysis and an MSGF scores $\leq 1 \times 10^{-10}$, which corresponded to an estimated false discovery rate (FDR) < 1% at the peptide level, were used to generate an accurate mass and time (AMT) tag database.[26] Matched peptide features from each data set were then filtered on a FDR of ≤ 5% using the statistical tools for AMT tag confidence metric.[27]

Peptide data quality control steps were performed to select for peptides of ABP-labeled proteins with significantly higher abundance compared to NA control peptides, identify outliers for removal, and normalize prior to peptide to protein roll-up. First, peptide AMT data for samples treated with ABPs and NADPH were compared to NA controls. To do this, peptides that were significant by g-test ($p < 0.05$)[28] and by *t* test (≥2-fold change) were retained and NA control runs were removed. Next, a standard outlier algorithm for proteomics was used RMD-PAV,[29] and Pearson correlation plots were implemented to identify outliers; resulting outliers were then removed. Lastly, the data were normalized using a percentage of peptide present (PPP) approach with a threshold of 25%.[30] Peptide AMT abundance values were then rolled up to proteins using RRollup[31] with criteria set to include that ≥3 peptides per protein were required for Grubb's test ($p < 0.05$), and only peptides unique to a single protein were utilized to estimate protein abundances. The resulting protein AMT abundance values were log2 transformed.

Activity-Based Proteomic Data Statistical Analysis. The primary goal for statistical analysis was to compare probe labeled protein AMT values for the exposure groups to those of the control SD-NoCSE group to understand the individual and combined effects of diet and smoking on P450 activity. To start, protein data normalization was performed using a standard reference-based normalization method to estimate protein abundances.[32,33] Next, quantitative differences of each of the five groups tested against the SD-NoCSE control data were calculated using analysis of variance (ANOVA) and Tukey test. Qualitative trends for exposure groups compared to SD-NoCSE controls were established using g-test, which evaluates the null hypothesis that the data are missing at random.[34] G-test results were then corrected for multiple comparisons with Bonferroni test. Proteins with *p*-values <0.05 were considered to have significantly different activity levels compared to the SD-NoCSE group.

Statistical analysis of the diet and smoke coexposure interaction on activity was performed using 2-way ANOVA (Prism7 software) corrected for multiple comparisons with a Bonferroni test; P450 with *p*-values <0.05 were considered to have activity significantly altered by the diet and smoke variable interaction term. For this analysis, only NoCSE and ACSE samples were evaluated.

RESULTS

Exposure Characterization. Male mice (C57Bl6/J) were fed a high fat diet (HFD) with ∼60% fat, or a standard fat diet (SD) with ∼13% diet. The HFD mice achieved an average weight ∼21% heavier than the corresponding SD mice after 11 weeks on the diets (Figure 2). The HFD mice from The Jackson Laboratory are a model for pre-T2DM, having increased body weights, elevated blood glucose, and impaired glucose tolerance.[35] Blood serum glucose was measured for each animal to assess glucose absorption at terminal necropsy. On average, there is a 45%, 47%, and 57% difference in serum glucose levels in NoCSE, PCSE, and ACSE, respectively, when compared to the SD-NoCSE group (Figure 2).

A cigarette smoking machine modified to simultaneously generate smoke streams that mimic active and passive smoking within designated chamber ports was utilized for exposing mice to active or passive cigarette smoke or filtered air (NoCSE). The dose targets for ACSE (250 WTPM/L; 250 ppm of CO) and PCSE (85 WTPM/L; 250 ppm of CO) were based upon levels determined by previous studies.[14] Actual delivered doses were maintained within 10% of each target, for example, 254.9 ± 10.6 WTPM/L for ACS and 82.0 ± 6.7 WTPM/L for PCS, with associated CO levels of 251.2 ± 6.6 ppm and 276.1 ± 8.8 ppm, respectively. All CSE mice exhibited significantly increased blood carboxyhemoglobin (COHb) levels relative to the NoCSE control mice, whereas the COHb levels were nearly the same for ACSE and PCSE mice and not statistically different in the HFD mice (Table 1).

P450 Activity Profiles. We applied ABP (Figure 1) to lung and liver microsomes. The ABP react mechanistically and irreversibly with individual functionally active P450 from nearly all P450 subfamilies. Resulting ABP labeled P450 were enriched and measured by high resolution LC−MS (Figure 1). To probe label microsomes, samples were treated with the requisite reducing cofactor, NADPH,[12] and null activity (NA) controls were also prepared as either heat-denatured (lung) or probe alone (without NADPH; liver). Active samples had significantly higher peptide abundances (g-test ($p < 0.05$); *t* test ($p < 0.05$); fold change ≥ 2) when statistically compared to peptides from NA controls, and retained for further data analysis and calculation of protein abundance values. In total, not accounting for exposures, the significant probe-labeled P450 compared to controls include 33 from liver samples and 13 from lung samples (Figure 3A and B, respectively).

Exposure-Dependent Alterations in Hepatic and Pulmonary P450 Activity. Statistical analysis of P450 activity profiles from individual exposures (PCSE-SD, ACSE-SD, and NoCSE-SD groups) and dual exposures (PCSE-HFD and ACSE-HFD groups) compared to the control NoCSE-SD group was performed. Statistically different (ANOVA $p < 0.05$, g-test $p < 0.05$) P450 activity levels for each comparison are shown in Figure 3C and D. In general, hepatic P450 activity levels decreased for HFD groups and increased with CSE, except for the ACSE-HFD group, which had activity increase for 1/3 of all identified enzymes and three with decreased activity. Conversely, lung profiles show that a HFD alone had very little effect while P- and ACSE resulted in increased activity for enzymes primarily involved in xenobiotic metabolism, except P450 2s1 and P450 20a, enzymes still yet to be classified for their function, and P450 39a1 which metabolizes oxycholesterol. Notable exceptions to the general exposure trends were for liver P450 2e1, which had increased activity for all HFD and CSE groups, whereas P450 2f2 displayed inverse changes in activity. In the lung, P450 2e1 was not identified, but P450 2f2 and 2s1 were significantly increased by CSE and decreased by HFD for all groups with a high degree of similarity. A striking finding is that the HFD resulted in decreased P450 39a1 in the liver, but increased activity in the lung. Additionally, it is important to point out that aside from P450 2e1, a HFD resulted in significantly decreased activity for the major xenobiotic metabolizing P450 including 1a2 and 3a11, highlighting the effect HFD has on DME function in the liver. Conversely, HFD exposure resulted in less P450 activity variance for the lung than in the liver data, but all CSE exposures resulted in increased P450 activity when compared to NoCSE-SD group. A HFD alone had no significant effect on P450 activity in the lung, but when combined with PCSE and ACSE, HFD did appear to be influential. The P450 20a, 4v2, 1a1, 2a5, 2d26, 2d11, and 39a1 were only identified for CSE

DOI: 10.1021/acs.chemrestox.8b00008
Chem. Res. Toxicol. 2018, 31, 308−318

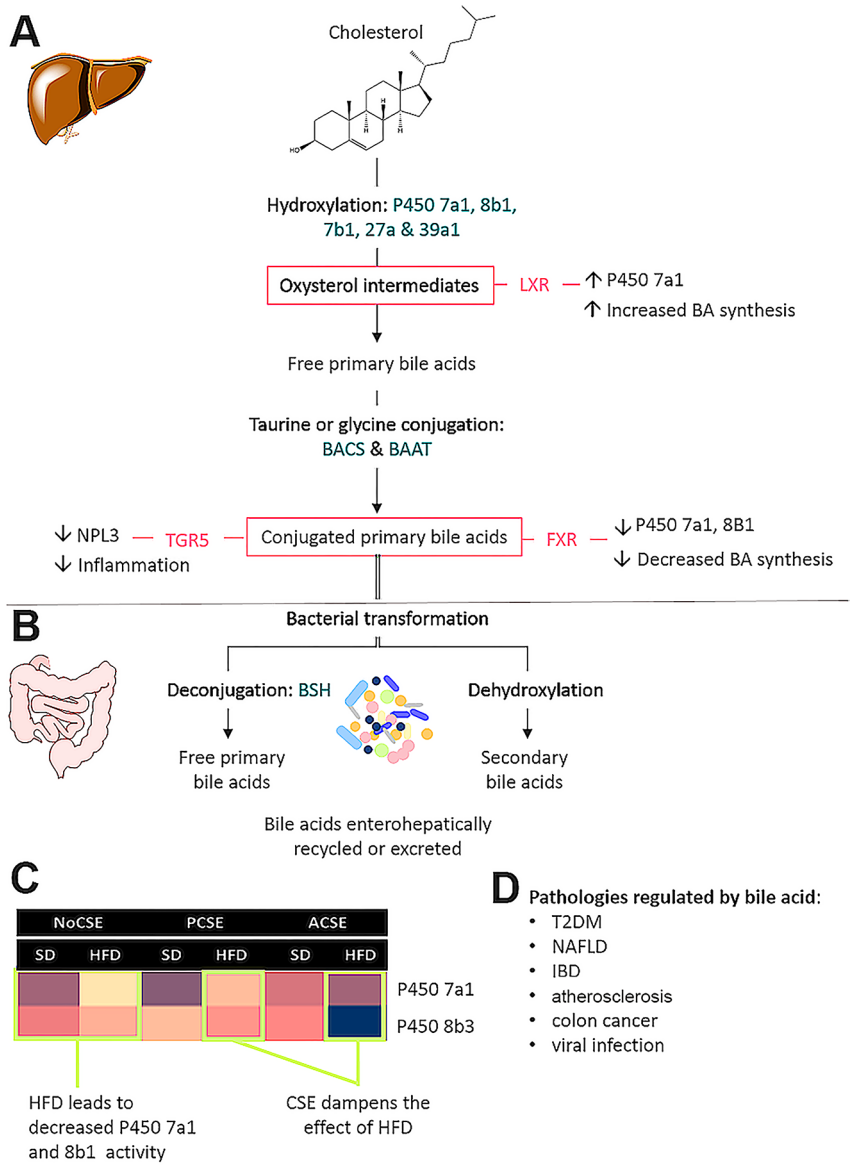

Figure 4. Bile acid synthesis and regulation. (A) Hepatic metabolism of cholesterol to bile acids. Key enzymes involved in bile acid synthesis, metabolites that function as nuclear receptor ligands (outlined in pink), corresponding nuclear receptor (pink text) and their regulatory effects. (B) Once conjugated, primary bile acids reach the intestinal tract via gallbladder, the microbiome transforms BA prior to enterohepatic cycling or excretion. (C) Heatmap view of HFD and CSE effect on P450 7a1 and 8b1 (details in Figure 3A with the exception that data presented here is Z-scaled). (D) List of pathologies regulated by BA. Abbreviations: BAAT; BSH, bile acid hydrolase; BACS, bile acid CoA synthase; BAAT, bile acid CoA–amino acid N-acetyltransferase; FXR, Farnesoid X receptor; LXR, Liver X receptor; IBD, Irritable Bowel Syndrome; T2DM, Type 2 Diabetes Mellitus.

groups. The P450 with significantly increased activity unique to PCSE-SD and ACSE-SD includes 2a5, 2d11, and 20a1 (Figure 3B).

The diet and smoke smoke interaction effect on P450 activity was statistically tested by two-way ANOVA with Bonferonni correction. The variables tested for diet were HFD and SD, and smoke variable only included NoCSE and ACSE data for liver and lung P450. For the liver samples, 16 P450 resulted in $p < 0.05$ while only one P450, 2s1 was very significantly effected by diet and smoke interaction. The significantly effected P450 and corresponding p-values are depicted in Figure 3E.

DISCUSSION

Diet-induced obesity and cigarette smoke are associated with oxidative stress, inflammation, and increased risk for disease,[36] and there is growing evidence that obesity can increase the risk of drug induced liver injury.[4,37] Our ABPP approach shows that HFD, passive and active CSE create significant, yet variable, impacts on P450 activity with tissue level disparity. In general, we find that HFD alone decreases activity for many P450 and alters the susceptibility of P450 to a secondary exposure, while CSE significantly increases activity levels for many xenobiotic metabolizing P450. It is also clear that a HFD together with ACSE lead to dramatic differences in P450 activity levels compared to individual exposures (Figure 3A–D), and that diet and CSE interaction significantly effects a subset of P450, including those key to drug metabolism (P450 3a11) and bile acid metabolism (P450 3a11,7a1, 7b1, 2c70), and lung P450 2s1 activity indicationg that these enzymes are susceptible to exposure interactions. We will discuss the exposure impacts of

DOI: 10.1021/acs.chemrestox.8b00008
Chem. Res. Toxicol. 2018, 31, 308–318

enzymes that play critical roles in drug, bile acid, and eicosanoid metabolism.

Concomitant Exposure to HFD and CS Leads to Highly Variable Activity Flux for Critical Drug Metabolizing P450. The metabolism of 95% of reported chemicals is enzymatically oxidized by P450,[11] and P450 families 1−3 are implicated in the metabolism of most xenobiotics, including 70−80% of all drugs in clinical use.[11,16] Therefore, understanding the impacts of common exposures on the functions of these enzymes is critical to determining personalized therapeutic dose and toxicity risk. The P450 1a1, 1a2, 1b1, and potentially 2s1 are inducible by the aryl hydrocarbon receptor (AHR) transcription factor; AHR ligands include many xenobiotics, tryptophan metabolites, and microbiota-derived compounds.[38,39] Our data show that CSE increases liver and lung P450 1a2 activity and lung P450 1a1 (ACSE > PCSE > NoCSE for SD and HFD groups), but HFD dampens this effect (Figure 3A). P450 2s1 is still classified as an "orphan enzyme" because a primary substrate has not been confirmed; however, Bui and colleagues demonstrated that benzo[*a*]-pyrene (BaP), the major cigarette smoke procarcinogen, AHR ligand, and P450 1a1 substrate, could be oxidized by human P450 2S1 to the highly carcinogenic (+)BaP-7,8-epoxide with support from NADPH or fatty acid hydroperoxides.[40] Additionally, this enzyme is highly expressed in hypoxic tumor cells and can perform reductive activation of the anticancer prodrug AQ4N.[41] There are significant and tissue specific HFD and CSE effects on family 2 P450 (Figure 3A−D). Our results indicate that compared to SD-NoCSE group, all HFD and CSE groups have significantly increased P450 2e1 activity. Induction studies show that when activated, this enzyme produces ROS, which in turn depletes concentrations of the cellular antioxidant glutathione and induces a pro-inflammatory cytokine storm,[42] pathologies associated with HFD and CSE. Additionally, P450 2f2 is responsible for activating a number chemicals, including the cigarette constituent naphthalene, to toxic metabolites in mice.[43] Our data show all CSE groups had significantly decreased liver P450 2f2 activity but increased lung activity (Figure 3A,C). P450 2a5, 2b, 2f, 2s have been shown to be involved in lung tumorigenesis in mice,[44] so observing increased activity for the enzymes by CSE exposure is not surprising, but that we see a HFD increasing activity as well indicates that diet may lead to increased risk for lung carcinogenesis when combined with CSE.

The P450 3a subfamily is the most prolific DME, but is also involved in metabolizing endogenous substrates.[11,45] Human P450 3A4 is responsible for the biotransformation of approximately 50% of therapeutic drugs currently on the market.[46] In mice, P450 3a11 is 76% homologous to human P450 3A4 and functions similarly.[47] Studies have shown that HFD, obesity and T2DM are associated with a significant decrease in hepatic P450 3A4 enzymatic activity and protein abundance in human liver microsome,[48,49] and a recent study found that inflammation results in down-regulation of P450 3a11 in mice.[50] Our data complement these findings and demonstrate that HFD-induced obesity results in significantly decreased hepatic P450 3a11 activity (Figure 3A,C) and that the diet and CSE interaction affected activity more than all P450 except 2c59. Altered P450 3A activity is clinically relevant for obese and diabetic patients with various comorbidities that require multiple medications. In general, our ABPP data indicate that a HFD negatively influences the functional capacity of xenobiotic metabolizing P450, which could lead to complications in pharmaceutical dosing and increased risk for hepatotoxicity.[5,6]

HFD-Induced Obesity Leads to Decreased Functional Capacity for Bile Acid Synthesis and Oxysterol Detoxification. Bile acid (BA) concentrations are regulated by the liver, GI tract, and gut microbiota (Figure 4). Though it was originally thought that the roll of BA was to simply aid in lipid digestion, it is now established that BA also function as signaling molecules involved in regulating energy homeostasis and concentrations of triglycerides, and glucose.[51−54] Recent studies agree that HFD induced obesity is accompanied by redox imbalance, inflammation, altered gut microbiome, and BA concentrations.[55,56] Except for P450 3a11 and 2c70, the HFD imposed reduction on BA metabolizing P450 was insignificant, yet the diet and smoke coexposure effect on liver P450 3a11, 2c70, 7a1, and 8b1 was significant (Figure 3E) indicating that this pathway may be susceptible to complex exposures and the impacts could lead to altered BA levels and therefore cellular signaling events across multiple organs.[55,56] Specific examples of a BA signaling network include the BA activated nuclear receptor farnesoid X receptor (FXR), which represses expression of *CYP7a1* and *CYP8b1*,[57] the products of which perform the first steps in converting cholesterol to CDCA and cholic acid respectively, but conjugated muricholic acid is an extremely potent FXR antagonist (Sayin et al.). Additionally, BA and FXR have been implicated as having inhibitory effects on NLRP3 inflammasome, which is associated with chronic inflammation in metabolic disorders.[53,54] Our data show that a HFD leads to repressed capacity for conversion of cholesterol to BA, which could be in part responsible for unresolved inflammation in obesity and associated pathologies.

A standout finding, which to our knowledge has not been previously reported, is for the significant impact CSE had on the activity of liver and lung P450 39a1, a hydroxylase selective for 24-hydroxycholesterol (24-HC). Our data show that P450 39a1 activity is significantly decreased for CSE groups in the liver but is significantly increased in the lung (Figure 3A−D). In the brain, P450 46a1 oxidizes cholesterol to 24-HC, which unlike cholesterol, can pass the blood−brain barrier to be selectively metabolized by P450 39a1. In healthy individuals, oxysterol levels are low and function as agonists for the nuclear transcription factor Liver X receptor (LXR) (Figure 4), a key regulator of cholesterol, fatty acid, and glucose homeostasis. However, increased oxysterol levels result in oxidative stress and are connected to human pathologies and influence carcinogenesis and cancer progression.[58] Recent metabolite studies found that obesity does not alter 24-HC plasma levels[59] but that CSE does and can be used as an oxidative stress biomarker for smokers.[60] Our ABPP results led us to speculate upon whether decreased liver P450 39a1 activity in CSE groups create bottlenecks in 24-HC detoxification, whereas significantly increased lung P450 39a1 may indicate a tissue specific activation of P450 39a1 functioning to protect the lung from CSE induced oxidative damage and inflammation. The missing functional link between circulating and target tissue oxysterols remains obscure,[58] but the clinical relevance requires follow-up studies.

Diet-Induced Obesity and CSE Result in Disparate Yet Significant Impacts on Activity of P450 Involved in Eicosanoid Metabolism and Lipid Detoxificatoion. Chemical or mechanical stress lead to an influx of inflammatory cytokines, signaling molecules that elicit marked changes in liver gene expression leading to downregulation of many DME,

DOI: 10.1021/acs.chemrestox.8b00008
Chem. Res. Toxicol. 2018, 31, 308−318

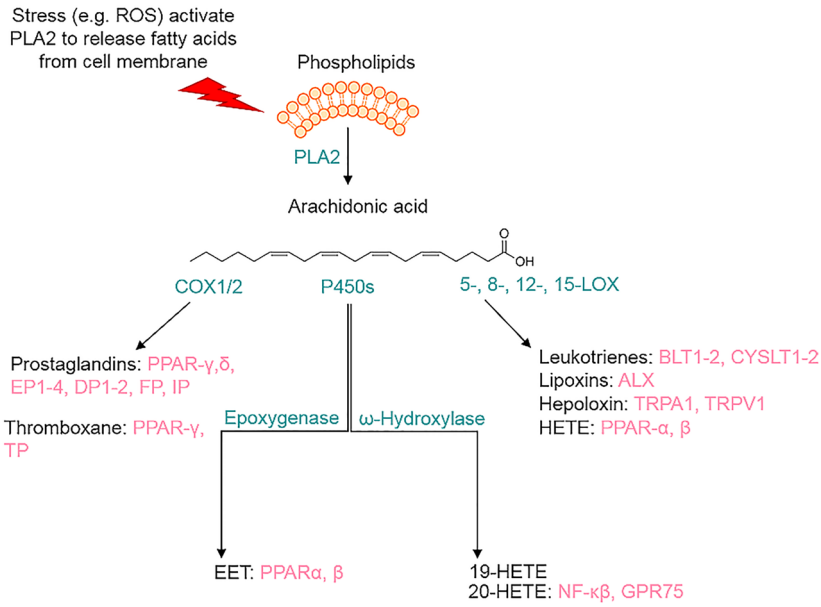

Figure 5. Stress induced eicosanoid synthesis. General overview of stress-induced activation of phospholipase A_2 (PLA_2) to release arachidonic acid from the cell membrane, and the varied metabolic pathways where arachidonic acid is converted to eicosanoids including cyclooxygenase-1 and -2 (COX1/2), 5-, 8-, 12-, and 15-lipoxygenases (5-, 8-, 12-, 15-LOX), and cytochrome P450 epoxyhydrolase and ω-hydroxylase (green text). Eicosanoid species (black text) and proposed receptors (pink text). Abbreviations: ALX, COX, cyclooxygenase; P450, cytochrome P450; EET, epoxyeicosatrienoic acid; GPR, G protein-coupled receptor; HETE, hydroxyeicosatetraenoic acid; HX, hepoxilin; LOX, lipoxygenase; LX, lipoxin; PLA2, phospholipase A2; PPAR, peroxisome proliferator-activated receptor; TRPA1, transient receptor potential ankyrin 1; TRPV1, transient receptor potential vanilloid 1; and TX, thromboxane.

yet the origin of this event is unclear.[61] The immune response involves complex molecular signaling networks with pro-inflammatory, anti-inflammatory, and pro-resolution functions coordinated by cytokine and eicosanoid biochemical messengers. Eicosanoids are signaling molecules derived from arachidonic acid (AA) with anti- or pro-inflammatory effects. The cyclooxygenase (COX) and lipoxygenase (LOX) arachidonic acid metabolites (Figure 5) have been studied extensively, whereas the P450 AA metabolites have not. The P450 epoxygenases, subfamilies 2c and 2j, convert AA to EET and are generally thought to function as agents in anti-inflammatory processes as evidenced by their ability to inhibit inflammatory cytokines.[62] Examples include 11,12-EET, which activates anti-inflammatory functions by binding peroxisome proliferator-activated receptor α (PPARα), while 11,12-EET and 8,9-EET exert anti-inflammatory effects by inhibiting endothelial nuclear factor-κB (NF-κB).[63] The P450 ω-hydroxylases, 4a and 4f metabolize AA to pro-inflammatory 20-HETE, P450 1a and 2e1 metabolize AA to 19-HETE and prostaglandins to malondialdehyde.[64] Here we show that compared to SD fed mice, HFD fed mice had decreased AA metabolizing P450 activity, with exception of P450 4f14, 4b1, and 2e1. Conversely, the combined exposure of ACSE and HFD leads to increased P450 1a2, 2c40, and 2c54 activity (Figure 3A,C). Fatty acid metabolizing P450 effected by diet and smoke interaction can be seen in Figure 3E.

Human P450 2B6, 3A4, 1A2, 2J2, and mouse 2c29 have been screened and shown to be responsible for the detoxification of α,β-unsaturated aldehydes lincluding 4-hydroxy-nonenal (4-HNE), a reactive biomolecule produced during lipid peroxidation. Oxidative stress can lead to accumulated 4-HNE, which forms critically harmful nucleic acid, protein, and memebrane lipid adducts and is associated with the onset of diabetes, cancer, cardiovascular, and neurodegenerative diseases.[65] A HFD dramatically decreased the activity of P450 1a2, 3a11, and 2c29 (Figure 3C) and the latter two enzymes were the most significantly effected by diet−smoke interaction (Figure 3E). A decreased capacity to detoxify reactive organic molecules would lead to increased risk for developing disease.

Mechanisms for constitutive and inducible regulation of P450 expression and activity are diverse and difficult to determine.[16] Altered P450 activity levels have the potential to increase susceptibility to toxicity, oxidative stress, and inflammation and in turn can result in a variety of pathologies. Our ABPP results show that HFD leads to significantly reduced functional capacity of many P450 involved in drug metabolism, signaling molecule synthesis, and reactive biomolecule detoxification. There are many xenobiotic-inducible mechanisms for modulating P450 expression and activity, and many have reported that inflammation by way of proinflammatory cytokine (e.g., interleukin-6) decrease P450 activity.[63] Inflammation accompanies obesity, so the widespread decrease in P450 activity we measured in HFD mice can likely be attributed to cytokine signaling events. On the other hand, the effects of cigarette smoke, an exposure also associated with inflammation, impacted the activity of only a few P450 in SD mice, whereas coexposure to cigarette smoke and HFD lead to many significantly increased P450. Future research should focus on the interaction, whether null, agonistic, or antagonistic, between inflammation and xenobiotics on cell signaling and P450 activity modulation. This understanding will be key to determining appropriate drug dosage for patients with conditions that are intrinsically linked to chronic inflammation and could even lead to therapeutic strategies for modulating dysregulated P450 activities caused by inflammatory events.

DOI: 10.1021/acs.chemrestox.8b00008
Chem. Res. Toxicol. 2018, 31, 308−318

■ ASSOCIATED CONTENT

Supporting Information

The Supporting Information is available free of charge on the ACS Publications website at DOI: 10.1021/acs.chemrestox.8b00008.

Log2 transformed AMT tag LC−MS values for activity-based probe labeled cytochrome P450 from liver and lung microsomes (XLSX)

■ AUTHOR INFORMATION

Corresponding Author

*E-mail: Aaron.Wright@pnnl.gov. Phone: (509) 372-5920.

ORCID

Aaron T. Wright: 0000-0002-3172-5253

Funding

This research was supported by the US National Institutes of Health, National Institute of Environmental Health Sciences under Grant Nos. P42 ES016465 and U54 ES016015. This work also used instrumentation and capabilities developed under support from the National Institute for General Medical Sciences (P41 GM103493). A portion of the research was performed in the Environmental Molecular Sciences Laboratory, a US Department of Energy Biological and Environmental Research national scientific user facility at Pacific Northwest National Laboratory (PNNL). PNNL is a multiprogram laboratory operated by Battelle for the US DOE under Contract No. DE-AC05−76RL01830.

Notes

The authors declare no competing financial interest.

■ REFERENCES

(1) WHO. (2014) *Global Status Report on Noncommunicable Diseases 2014*, World Health Organization, Geneva.

(2) Heindel, J. J., Blumberg, B., Cave, M., Machtinger, R., Mantovani, A., Mendez, M. A., Nadal, A., Palanza, P., Panzica, G., Sargis, R., Vandenberg, L. N., and vom Saal, F. (2017) Metabolism disrupting chemicals and metabolic disorders. *Reprod. Toxicol. 68*, 3−33.

(3) Tarantino, G., Conca, P., Basile, V., Gentile, A., Capone, D., Polichetti, G., and Leo, E. (2007) A prospective study of acute drug-induced liver injury in patients suffering from non-alcoholic fatty liver disease. *Hepatol. Res. 37*, 410−415.

(4) Michaut, A., Moreau, C., Robin, M. A., and Fromenty, B. (2014) Acetaminophen-induced liver injury in obesity and nonalcoholic fatty liver disease. *Liver Int. 34*, e171−179.

(5) Cheymol, G. (2000) Effects of obesity on pharmacokinetics implications for drug therapy. *Clin. Pharmacokinet. 39*, 215−231.

(6) Hanley, M. J., Abernethy, D. R., and Greenblatt, D. J. (2010) Effect of obesity on the pharmacokinetics of drugs in humans. *Clin. Pharmacokinet. 49*, 71−87.

(7) Carmody, R. N., Gerber, G. K., Luevano, J. M., Jr., Gatti, D. M., Somes, L., Svenson, K. L., and Turnbaugh, P. J. (2015) Diet dominates host genotype in shaping the murine gut microbiota. *Cell Host Microbe 17*, 72−84.

(8) Kobyliak, N., Conte, C., Cammarota, G., Haley, A. P., Styriak, I., Gaspar, L., Fusek, J., Rodrigo, L., and Kruzliak, P. (2016) Probiotics in prevention and treatment of obesity: a critical view. *Nutr. Metab. 13*, 14.

(9) Swanson, H. I. (2015) Drug Metabolism by the Host and Gut Microbiota: A Partnership or Rivalry? *Drug Metab. Dispos. 43*, 1499−1504.

(10) Erstad, B. L. (2017) Improving Medication Dosing in the Obese Patient. *Clin. Drug Invest. 37*, 1−6.

(11) Rendic, S., and Guengerich, F. P. (2015) Survey of Human Oxidoreductases and Cytochrome P450 Enzymes Involved in the Metabolism of Xenobiotic and Natural Chemicals. *Chem. Res. Toxicol. 28*, 38−42.

(12) Nelson, D. R., Zeldin, D. C., Hoffman, S. M., Maltais, L. J., Wain, H. M., and Nebert, D. W. (2004) Comparison of cytochrome P450 (CYP) genes from the mouse and human genomes, including nomenclature recommendations for genes, pseudogenes and alternative-splice variants. *Pharmacogenetics 14*, 1−18.

(13) Guengerich, F. P. (2017) Intersection of the Roles of Cytochrome P450 Enzymes with Xenobiotic and Endogenous Substrates: Relevance to Toxicity and Drug Interactions. *Chem. Res. Toxicol. 30*, 2−12.

(14) Obot, C., Lee, K., Fuciarelli, A., Renne, R., and McKinney, W. (2004) Characterization of mainstream cigarette smoke-induced biomarker responses in ICR and C57Bl/6 mice. *Inhalation Toxicol. 16*, 701−719.

(15) Kawada, T., Otsuka, T., Endo, T., and Kon, Y. (2011) The metabolic syndrome, smoking, inflammatory markers and obesity. *Int. J. Cardiol. 151*, 367−368 author reply 373−364..

(16) Zanger, U. M., Klein, K., Thomas, M., Rieger, J. K., Tremmel, R., Kandel, B. A., Klein, M., and Magdy, T. (2014) Genetics, epigenetics, and regulation of drug-metabolizing cytochrome p450 enzymes. *Clin. Pharmacol. Ther. 95*, 258−261.

(17) Hrycay, E. G., and Bandiera, S. M. (2009) Expression, function and regulation of mouse cytochrome P450 enzymes: comparison with human P450 enzymes. *Curr. Drug Metab. 10*, 1151−1183.

(18) Sadler, N. C., Nandhikonda, P., Webb-Robertson, B. J., Ansong, C., Anderson, L. N., Smith, J. N., Corley, R. A., and Wright, A. T. (2016) Hepatic Cytochrome P450 Activity, Abundance, and Expression Throughout Human Development. *Drug Metab. Dispos. 44*, 984−991.

(19) Perez, D. M., Richards, M. P., Parker, R. S., Berres, M. E., Wright, A. T., Sifri, M., Sadler, N. C., Tatiyaborworntham, N., and Li, N. (2016) Role of Cytochrome P450 Hydroxylase in the Decreased Accumulation of Vitamin E in Muscle from Turkeys Compared to that from Chickens. *J. Agric. Food Chem. 64*, 671−680.

(20) Wright, A. T., and Cravatt, B. F. (2007) Chemical proteomic probes for profiling cytochrome p450 activities and drug interactions in vivo. *Chem. Biol. 14*, 1043−1051.

(21) Wright, A. T., Song, J. D., and Cravatt, B. F. (2009) A suite of activity-based probes for human cytochrome P450 enzymes. *J. Am. Chem. Soc. 131*, 10692−10700.

(22) Ismail, H. M., O'Neill, P. M., Hong, D. W., Finn, R. D., Henderson, C. J., Wright, A. T., Cravatt, B. F., Hemingway, J., and Paine, M. J. (2013) Pyrethroid activity-based probes for profiling cytochrome P450 activities associated with insecticide interactions. *Proc. Natl. Acad. Sci. U. S. A. 110*, 19766−19771.

(23) Crowell, S. R., Sharma, A. K., Amin, S., Soelberg, J. J., Sadler, N. C., Wright, A. T., Baird, W. M., Williams, D. E., and Corley, R. A. (2013) Impact of pregnancy on the pharmacokinetics of dibenzo-[def,p]chrysene in mice. *Toxicol. Sci. 135*, 48−62.

(24) Renaud, H. J., Cui, J. Y., Khan, M., and Klaassen, C. D. (2011) Tissue distribution and gender-divergent expression of 78 cytochrome P450 mRNAs in mice. *Toxicol. Sci. 124*, 261−277.

(25) Kim, S., Gupta, N., and Pevzner, P. A. (2008) Spectral probabilities and generating functions of tandem mass spectra: a strike against decoy databases. *J. Proteome Res. 7*, 3354−3363.

(26) Zimmer, J. S., Monroe, M. E., Qian, W. J., and Smith, R. D. (2006) Advances in proteomics data analysis and display using an accurate mass and time tag approach. *Mass Spectrom. Rev. 25*, 450−482.

(27) Stanley, J. R., Adkins, J. N., Slysz, G. W., Monroe, M. E., Purvine, S. O., Karpievitch, Y. V., Anderson, G. A., Smith, R. D., and Dabney, A. R. (2011) A statistical method for assessing peptide identification confidence in accurate mass and time tag proteomics. *Anal. Chem. 83*, 6135−6140.

(28) Webb-Robertson, B. J., McCue, L. A., Waters, K. M., Matzke, M. M., Jacobs, J. M., Metz, T. O., Varnum, S. M., and Pounds, J. G. (2010) Combined statistical analyses of peptide intensities and peptide

DOI: 10.1021/acs.chemrestox.8b00008
Chem. Res. Toxicol. 2018, 31, 308−318

occurrences improves identification of significant peptides from MS-based proteomics data. *J. Proteome Res. 9*, 5748−5756.
(29) Matzke, M. M., Waters, K. M., Metz, T. O., Jacobs, J. M., Sims, A. C., Baric, R. S., Pounds, J. G., and Webb-Robertson, B. J. (2011) Improved quality control processing of peptide-centric LC−MS proteomics data. *Bioinformatics 27*, 2866−2872.
(30) Wang, P., Tang, H., Zhang, H., Whiteaker, J., Paulovich, A. G., and McIntosh, M. (2006) Normalization regarding non-random missing values in high-throughput mass spectrometry data. *Pac Symp. Biocomput*, 315−326.
(31) Polpitiya, A. D., Qian, W. J., Jaitly, N., Petyuk, V. A., Adkins, J. N., Camp, D. G., 2nd, Anderson, G. A., and Smith, R. D. (2008) DAnTE: a statistical tool for quantitative analysis of -omics data. *Bioinformatics 24*, 1556−1558.
(32) Matzke, M. M., Brown, J. N., Gritsenko, M. A., Metz, T. O., Pounds, J. G., Rodland, K. D., Shukla, A. K., Smith, R. D., Waters, K. M., McDermott, J. E., and Webb-Robertson, B. J. (2013) A comparative analysis of computational approaches to relative protein quantification using peptide peak intensities in label-free LC−MS proteomics experiments. *Proteomics 13*, 493−503.
(33) Taverner, T., Karpievitch, Y. V., Polpitiya, A. D., Brown, J. N., Dabney, A. R., Anderson, G. A., and Smith, R. D. (2012) DanteR: an extensible R-based tool for quantitative analysis of -omics data. *Bioinformatics 28*, 2404−2406.
(34) Webb-Robertson, B. J., Wiberg, H. K., Matzke, M. M., Brown, J. N., Wang, J., McDermott, J. E., Smith, R. D., Rodland, K. D., Metz, T. O., Pounds, J. G., and Waters, K. M. (2015) Review, evaluation, and discussion of the challenges of missing value imputation for mass spectrometry-based label-free global proteomics. *J. Proteome Res. 14*, 1993−2001.
(35) Omar, B., Pacini, G., and Ahren, B. (2012) Differential development of glucose intolerance and pancreatic islet adaptation in multiple diet induced obesity models. *Nutrients 4*, 1367−1381.
(36) Esser, N., Legrand-Poels, S., Piette, J., Scheen, A. J., and Paquot, N. (2014) Inflammation as a link between obesity, metabolic syndrome and type 2 diabetes. *Diabetes Res. Clin. Pract. 105*, 141−150.
(37) Aubert, J., Begriche, K., Knockaert, L., Robin, M. A., and Fromenty, B. (2011) Increased expression of cytochrome P450 2E1 in nonalcoholic fatty liver disease: mechanisms and pathophysiological role. *Clin. Res. Hepatol. Gastroenterol. 35*, 630−637.
(38) Ma, Q., and Lu, A. Y. (2007) CYP1A induction and human risk assessment: an evolving tale of in vitro and in vivo studies. *Drug Metab. Dispos. 35*, 1009−1016.
(39) Liguori, M., Lee, C.-H., Liu, H., Ciurlionis, R., Ditewig, A., Doktor, S., Andracki, M., Gagne, G., Waring, J., Marsh, K., Gopalakrishnan, M., Blomme, E., and Yang, Y. (2012) AhR activation underlies the CYP1A autoinduction by A-998679 in rats. *Front. Genet. 3*, 1.
(40) Bui, P. H., Hsu, E. L., and Hankinson, O. (2009) Fatty acid hydroperoxides support cytochrome P450 2S1-mediated bioactivation of benzo[a]pyrene-7,8-dihydrodiol. *Mol. Pharmacol. 76*, 1044−1052.
(41) Nishida, C. R., Lee, M., and de Montellano, P. R. (2010) Efficient hypoxic activation of the anticancer agent AQ4N by CYP2S1 and CYP2W1. *Mol. Pharmacol. 78*, 497−502.
(42) Linhart, K., Bartsch, H., and Seitz, H. K. (2014) The role of reactive oxygen species (ROS) and cytochrome P-450 2E1 in the generation of carcinogenic etheno-DNA adducts. *Redox Biol. 3*, 56−62.
(43) Shultz, M. A., Choudary, P. V., and Buckpitt, A. R. (1999) Role of murine cytochrome P-450 2F2 in metabolic activation of naphthalene and metabolism of other xenobiotics. *J. Pharmacol Exp Ther 290*, 281−288.
(44) Li, L., Megaraj, V., Wei, Y., and Ding, X. (2014) Identification of cytochrome P450 enzymes critical for lung tumorigenesis by the tobacco-specific carcinogen 4-(methylnitrosamino)-1-(3-pyridyl)-1-butanone (NNK): insights from a novel Cyp2abfgs-null mouse. *Carcinogenesis 35*, 2584−2591.
(45) Marill, J., Cresteil, T., Lanotte, M., and Chabot, G. G. (2000) Identification of human cytochrome P450 involved in the formation of all-trans-retinoic acid principal metabolites. *Mol. Pharmacol. 58*, 1341−1348.
(46) Nebert, D. W., and Russell, D. W. (2002) Clinical importance of the cytochromes P450. *Lancet 360*, 1155−1162.
(47) Yanagimoto, T., Itoh, S., Muller-Enoch, D., and Kamataki, T. (1992) Mouse liver cytochrome P-450 (P-450IIIAM1): its cDNA cloning and inducibility by dexamethasone. *Biochim. Biophys. Acta, Gene Struct. Expression 1130*, 329−332.
(48) Kotlyar, M., and Carson, S. W. (1999) Effects of obesity on the cytochrome P450 enzyme system. *Int. J. Clin Pharmacol Ther 37*, 8−19.
(49) Dostalek, M., Court, M. H., Yan, B., and Akhlaghi, F. (2011) Significantly reduced cytochrome P450 3A4 expression and activity in liver from humans with diabetes mellitus. *Br. J. Pharmacol. 163*, 937−947.
(50) Gross, B., Pawlak, M., Lefebvre, P., and Staels, B. (2017) PPARs in obesity-induced T2DM, dyslipidaemia and NAFLD. *Nat. Rev. Endocrinol. 13*, 36−49.
(51) Lefebvre, P., Cariou, B., Lien, F., Kuipers, F., and Staels, B. (2009) Role of bile acids and bile acid receptors in metabolic regulation. *Physiol. Rev. 89*, 147−191.
(52) Hao, H., Cao, L., Jiang, C., Che, Y., Zhang, S., Takahashi, S., Wang, G., and Gonzalez, F. J. (2017) Farnesoid X Receptor Regulation of the NLRP3 Inflammasome Underlies Cholestasis-Associated Sepsis. *Cell Metab. 25*, 856−867.e5.
(53) Guo, C., Xie, S., Chi, Z., Zhang, J., Liu, Y., Zhang, L., Zheng, M., Zhang, X., Xia, D., Ke, Y., Lu, L., and Wang, D. (2016) Bile Acids Control Inflammation and Metabolic Disorder through Inhibition of NLRP3 Inflammasome. *Immunity 45*, 802−816.
(54) Pathak, P., Liu, H., Boehme, S., Xie, C., Krausz, K. W., Gonzalez, F., and Chiang, J. Y. L. (2017) Farnesoid X receptor induces Takeda G-protein receptor 5 Crosstalk to regulate Bile Acid Synthesis and Hepatic Metabolism. *J. Biol. Chem. 292*, 11055.
(55) Wahlstrom, A., Sayin, S. I., Marschall, H. U., and Backhed, F. (2016) Intestinal Crosstalk between Bile Acids and Microbiota and Its Impact on Host Metabolism. *Cell Metab. 24*, 41−50.
(56) Ma, H., and Patti, M. E. (2014) Bile acids, obesity, and the metabolic syndrome. *Best Pract Res. Clin Gastroenterol 28*, 573−583.
(57) Sayin, S. I., Wahlstrom, A., Felin, J., Jantti, S., Marschall, H. U., Bamberg, K., Angelin, B., Hyotylainen, T., Oresic, M., and Backhed, F. (2013) Gut microbiota regulates bile acid metabolism by reducing the levels of tauro-beta-muricholic acid, a naturally occurring FXR antagonist. *Cell Metab. 17*, 225−235.
(58) Kloudova, A., Guengerich, F. P., and Soucek, P. (2017) The Role of Oxysterols in Human Cancer. *Trends Endocrinol. Metab. 28*, 485.
(59) Guillemot-Legris, O., Mutemberezi, V., Cani, P. D., and Muccioli, G. G. (2016) Obesity is associated with changes in oxysterol metabolism and levels in mice liver, hypothalamus, adipose tissue and plasma. *Sci. Rep. 6*, 19694.
(60) Seet, R. C., Lee, C. Y., Loke, W. M., Huang, S. H., Huang, H., Looi, W. F., Chew, E. S., Quek, A. M., Lim, E. C., and Halliwell, B. (2011) Biomarkers of oxidative damage in cigarette smokers: which biomarkers might reflect acute versus chronic oxidative stress? *Free Radical Biol. Med. 50*, 1787−1793.
(61) Slaviero, K. A., Clarke, S. J., and Rivory, L. P. (2003) Inflammatory response: an unrecognised source of variability in the pharmacokinetics and pharmacodynamics of cancer chemotherapy. *Lancet Oncol. 4*, 224−232.
(62) Node, K., Huo, Y., Ruan, X., Yang, B., Spiecker, M., Ley, K., Zeldin, D. C., and Liao, J. K. (1999) Anti-inflammatory properties of cytochrome P450 epoxygenase-derived eicosanoids. *Science 285*, 1276−1279.
(63) Zanger, U. M., and Schwab, M. (2013) Cytochrome P450 enzymes in drug metabolism: regulation of gene expression, enzyme activities, and impact of genetic variation. *Pharmacol. Ther. 138*, 103−141.
(64) Dennis, E. A., and Norris, P. C. (2015) Eicosanoid storm in infection and inflammation. *Nat. Rev. Immunol. 15*, 511−523.

DOI: 10.1021/acs.chemrestox.8b00008
Chem. Res. Toxicol. 2018, 31, 308−318

(65) Amunom, I., Dieter, L. J., Tamasi, V., Cai, J., Conklin, D. J., Srivastava, S., Martin, M. V., Guengerich, F. P., and Prough, R. A. (2011) Cytochromes P450 catalyze the reduction of alpha,beta-unsaturated aldehydes. *Chem. Res. Toxicol. 24*, 1223−1230.

DOI: 10.1021/acs.chemrestox.8b00008
Chem. Res. Toxicol. 2018, 31, 308−318